Journal of Cleaner Production 279 (2021) 123609

Contents lists available at ScienceDirect

Journal of Cleaner Production

journal homepage: www.elsevier.com/locate/jclepro

# An experimental investigation on energy-effective additive manufacturing of aluminum parts via process parameter selection

Tao Peng [a], Jingxiang Lv [b, c, *], Arfan Majeed [c], Xihui Liang [d]

[a] State Key Laboratory of Fluid Power and Mechatronic Systems, Key Laboratory of 3D Printing Process and Equipment of Zhejiang Province, School of Mechanical Engineering, Zhejiang University, Hangzhou, China
[b] Key Laboratory of Road Construction Technology and Equipment of MOE, School of Construction Machinery, Chang'an University, Xi'an, China
[c] Key Laboratory of Contemporary Design and Integrated Manufacturing Technology, School of Mechanical Engineering, Northwestern Polytechnical University, Xi'an, China
[d] Department of Mechanical Engineering, University of Manitoba, Winnipeg, Manitoba, R3T 5V6, Canada

ARTICLE INFO

*Article history:*
Received 6 November 2019
Received in revised form
13 June 2020
Accepted 3 August 2020
Available online 14 August 2020

Handling editor: Prof. Jiri Jaromir Klemeš

*Keywords:*
Selective laser melting
Parameter selection
Aluminum alloy
Mechanical property
Specific energy consumption

ABSTRACT

This paper investigates the influences of process parameters on part quality, electrical energy consumption, and corresponding energy effectiveness (EE) of AlSi10Mg specimens fabricated by selective laser melting (SLM). Here, EE is defined as the ratio between equivalent quality and specific energy consumption (SEC), where SEC refers to the energy consumption per kilogram of part produced during the building process. The reduction of electrical energy without significantly compromising quality via process parameter configuration was studied. Three parameters, laser power, scan speed and overlap rate, were selected and full factorial design was employed. Single track and single layer experiments were conducted to determine the ranges of process parameters, and multiple layer specimens were prepared for the testing of quality performances, including density, tensile strength, and hardness. The energy consumption of the auxiliary system and laser of the SLM machine were measured for SEC calculation. Results show that the density does not increase with increased SEC, while the tensile strength and hardness show increasing trends. EE can be improved without significantly sacrificing density and hardness, but the tensile strength will be greatly reduced. A case showed that a significant percentage (27.8%) of electrical energy could be saved while satisfying the quality requirements via proper selection of process parameters for the manufacturing of SLMed parts. The findings will help process designers to foster the sustainability of additive manufacturing.

© 2020 Elsevier Ltd. All rights reserved.

## 1. Introduction

Aluminum alloys own a series of excellent properties, such as lightweight, good elasticity, high tensile strength and stiffness, good corrosion and abrasion resistance, and good conductivity of heat and electricity (Zhang et al., 2019a). Due to decent manufacturability and recyclability, aluminum parts have been widely used in industrial applications, particularly aerospace and automotive industries, and the demand is exponentially increasing (Garavaglia et al., 2019). Forging, die casting, and machining processes are normally involved in fabricating a part, which heavily rely on energy-intensive equipment, such as large-scale furnace, forging and die casting machine, or machining center. This leads to huge energy consumption, severe pollution, and low material efficiency (Park et al., 2016).

Additive Manufacturing (AM), with its technological maturity, provides a promising alternative approach to free the part design, which in return, can fabricate complex structural and functional parts with improved performance (Aboulkhair et al., 2019). This possesses great potentials in many industries (Gao et al., 2015). The layer-wise additive nature of the process is often regarded as a cleaner and sustainable process, however, till now, such a claim is weakly supported by quantitative analysis. As recognized in existing researches, industrial sector accounts for nearly one third of the global energy consumption (EIA, 2016), and imposes tremendous environmental concerns. Energy issue has been studied for machining (Lv et al., 2019), casting (Zheng et al., 2018), grinding

* Corresponding author. Key Laboratory of Road Construction Technology and Equipment of MOE, School of Construction Machinery, Chang'an University, Xi'an, China.
*E-mail address:* lvjx@chd.edu.cn (J. Lv).

https://doi.org/10.1016/j.jclepro.2020.123609
0959-6526/© 2020 Elsevier Ltd. All rights reserved.

(Winter et al., 2014), and several other non-conventional processes (Peng and Chen, 2018). It has also been identified that energy consumption is gradually becoming an environmental constraint for the industrial adoption of AM technologies (Peng et al., 2018a). However, fundamental research on energy efficiency and savings of such emerging technologies is still lacking.

Based on existing AM studies (Zhu et al., 2019), energy savings is not a primary concern unless assuring specified quality/property requirements. Therefore, energy effectiveness (EE) is proposed as "a systematic method to minimize the total processing energy consumption in achieving the specifically detailed product quality/property requirements" (Peng et al., 2019b). However, it is challenging to quantify it due to various influential aspects, including part design, material specifications, and process parameters. Fig. 1 depicts the factors that influence the part quality and overall energy performance of AM processes, where the quantitative relationship between process parameters and EE remains undiscovered. In this paper, an experimental investigation to reveal this relationship has been conducted. Specific energy consumption (SEC) is adopted to facilitate energy calculation, which has been intensively used in existing studies on machining energy (Zeng et al., 2019). The selected mechanical properties of aluminum parts, including density, hardness and tensile strength, are used for quality/property requirements. To achieve energy-effective AM, we minimize processing energy consumption and meet the required mechanical properties via process parameter configuration in this research.

The remainder of the paper is organized in five sections. A literature survey on energy and quality in aluminum additive manufacturing was reported in Section 2. The experimental setup and experimental design are elaborated in Section 3, and results are presented in Section 4, followed by the limitation and potential applications discussed in Section 5. Finally, concluding remarks and outlooks are given in Section 6.

## 2. State-of-the-art

In this section, we present a brief overview of the existing research in the areas of energy consumption and part quality of AM processes, specifically, selective laser melting (SLM) processes.

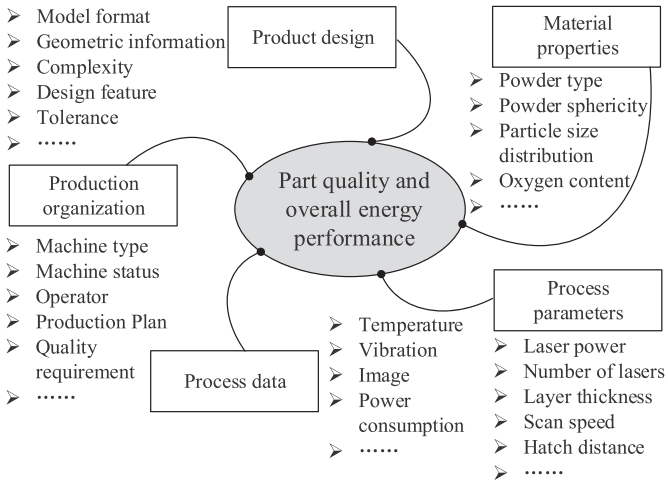


**Fig. 1.** Factors that influence the part quality and overall energy performance of AM processes. The EE is influenced by product design, material properties, process parameters, process data and production organization.

### 2.1. Energy consumption of the SLM processes

SLM is one of the most reliable AM processes for metal part fabrication with high accuracy, density and good surface finish (Ahmed, 2019). The SLM fabricated parts illustrate higher tensile strength, hardness, etc. than conventional manufactured objects, due to the certain metallurgical circumstances that are present during the process, such as fast solidification, directional heat flux, and temperature gradient, which permit ultrafine microstructures to be formed inside the final parts (Trevisan et al., 2017).

SLM can manufacture solid parts, honeycomb structures, porous structures, thin-walled parts, etc. in a wide range of materials, including titanium alloys, steel, and nickel alloys (Kruth et al., 2004; Sadowski et al., 2016; Tan et al., 2015). The aluminum alloys have developed great interests for the SLM process. AlSi10Mg is a traditional cast alloy, which is generally used for die-casting. This alloy has been extensively used in the automotive and aerospace industry, due to its high strength, good weldability, hardenability and good mechanical properties (Gupta et al., 2001).

There is a growing recognition of the potential advantages of SLM processes for enabling sustainable manufacturing through a reduced consumption of energy and materials. During SLM processing, energy is required to deliver feedstock material, obtain and maintain a proper thermal and atmospheric condition, power motors for positioning worktable and/or beam delivery systems, power laser beam for melting the material powders, and enable in-process sensors and controllers (Baumers et al., 2010). The energy consumption models of AM machine subsystems, including laser system, cooling system and motor drives were partially developed and validated through experiments (Bourhis et al., 2013).

There are two operational modes in a SLM process, non-productive and productive modes. The former consists of machine preparation, preheating, cooling down, and part retrieval stages. The latter covers power recoating and laser scanning stages (Kellens et al., 2014). As high as 68% time and 80% energy consumption in a SLM process can be attributed to laser scanning stage (Kellens et al., 2011). Yi et al. (2018) proposed an approach to predict the energy consumption of SLM based on physical modeling of the energetic behavior of machine components. Based on their method, a simulation tool for energy consumption prediction of SLM was later developed (Yi et al., 2019).

Specific energy consumption (SEC) is widely used for evaluating the energy consumption of manufacturing processes, including AM (Gutowski et al., 2006). The SEC of various AM technologies, including stereolithography (SLA) (Luo et al., 1999), selective laser sintering (SLS) (Baumers et al., 2011; Paul and Anand, 2012), laser cladding process (Peng et al., 2019a) and laser engineered net shaping (LENS) process (Liu et al., 2018b) has been studied. The energy consumption of SLM process is affected simultaneously by many process parameters, such as laser power, scan speed, hatch space and layer thickness (Lv et al., 2020). However, there is still a lack of study on the SEC of SLM processes.

### 2.2. Quality of the SLM fabricated parts

A wide range of materials, titanium alloys, aluminum alloys, steel, nickel alloys, etc., can be manufactured using SLM. Considering material energy absorption rate, oxidation, and residual stress, the fine control of process parameters in a rigorously protective environment is essential to ensure their formation quality. Many studies have investigated the influence of process parameters on SLMed part quality using experimental design and statistical analysis. Read et al. (2015) investigated the influence of laser power, scan speed, hatch distance, and island size on the porosity development of AlSi10Mg alloy. Jiang et al. (2019) comprehensively

studied the effects of laser power, scan speed, hatch distance and their interactions on surface roughness, hardness and density of SLM fabricated 316 L stainless steel parts. Zhang et al. (2019b) examined the effects of energy density, build orientation and location on the porosity and mechanical properties of Ti−6Al−4V alloy parts. Anwar and Pham (2017) studied the effects of laser scan direction, part placement and the flow velocity of inert gas on the tensile strength of AlSi10Mg parts. The effects of scan speed, layer thickness, and building direction on dimensional accuracy, surface roughness and mechanical properties of 316L stainless steel were investigated experimentally (Delgado et al., 2012). They reported that the tensile strength decreases as the layer thickness increases. While most studies were based on experiments, Zhang et al. (2018) theoretically modeled the horizontal dimensional accuracy as a function of track width, hatch space and solidification shrinkage. Based on their model, the dimension deviation of a thin-wall sample could be reduced to less than 20 μm using a pre-compensation method. Since part quality was greatly influenced by process parameters, it is important to select them appropriately.

### 2.3. Energy consumption and quality of the AM parts

While the above research focused on either energy consumption or part quality, multi-objective optimization studies on both, i.e. energy effectiveness, draws increasing interests. Ratnadeep and Sam (2015) obtained an optimized values of layer thickness and part orientation of metal powder AM processes to achieve lower energy consumption, lower dimensional errors and higher part strength. Strano et al. (2013) minimized the process energy and surface roughness for SLS by controlling build orientation and layer thickness. Majeed et al. (2019) proposed a big data driven framework to analyze and optimize energy consumption and product quality together. They found that energy consumption could be greatly reduced without compromising part quality.

Developing a mathematical model of part quality is challenging, due to the complexity of part formation process and in-process quality evolution mechanism. Alternatively, joint analysis on energy consumption and quality performances based on experimentation were normally employed. The influence of exposure time on energy consumption and mechanical properties of SLM fabricated parts was investigated, and it was found that the tensile strength and maximum torque were notably improved with increased energy consumption (Peng et al., 2018b). The correlation between energy consumption and mechanical properties were investigated, and the results showed that density can be improved without increasing energy consumption, but flexural strength was different (Zhu et al., 2019). However, in those study, only two parameters, laser power and exposure time, were considered. Other parameters, such as scan speed and overlap rate, were fixed. However, these parameters are related to SEC, thereby need to be studied towards energy-effective AM processes. In this paper, laser power, scan speed and overlap rate were experimentally investigated for their impacts on the part quality (i.e. relative density, tensile strength and hardness) and electrical energy consumption, to determine how electrical energy consumption can be effectively reduced without significantly compromising mechanical properties.

## 3. Experimental study

### 3.1. Experiment setup

Sample fabrication experiments were conducted on an SLM $280^{HL}$facility (SLM Solutions GmbH). Gas-atomized AlSi10Mg powders, proprietarily supplied, with particle size ranging from 20 μm to 50 μm were used. A Tescan VEGA 3 LMU Scanning Electron Microscope (SEM) was used to verify the particle size of the powders, as shown in Fig. 2. Table 1 shows its chemical compositions. Before the powder was used in fabrication, it was dried in an oven at the temperature of 100 °C.

The quality of fabricated samples and the electrical energy consumption of the SLM machine were measured in our laboratory. An optical inverted metallurgical microscope (Olympus GX51) with built-in front camera port was employed to observe the surface morphology, and measure the width of the single-track samples at the magnification of 100. The relative density of the samples was measured using the Archimedes' principle, where a balance of Sartorius BS 124S with an accuracy of ±0.10 mg was used. The mass of each sample was measured three times in both air and water. The relative density of the sample was calculated as (Perevoshchikova et al., 2017):

$$\rho_{RD} = \frac{\rho_p}{\rho_t} \times 100\% \tag{1}$$

where:

$$\rho_p = (\rho_{water} - \rho_{air}) \frac{m_a}{m_a - m_{water}} + \rho_{air} \tag{2}$$

where $\rho_p$is the density of a tested sample; the theoretical density of an AlSi10Mg part $\rho_t$ is 2.68 g/cm$^3$ (Bai et al., 2019); the density of air $\rho_{air}$ at 20 °C and 1 atm is 1.2754 kg/m$^3$; the water density $\rho_{water}$ at 20 °C is 998.2 kg/m$^3$; $m_a$ and $m_{water}$ are the mass of a sample in air and water [gram], respectively. Tensile strength was measured on an electromechanical universal testing machine made by Instron. For Vickers hardness test, a Leco AMH 43 automatic hardness tester was used with a load force of 0.49 N and a dwell time of 10 s. For hardness testing, each experiment was repeated five times, and the average value was taken.

For energy measurement, a power acquisition system, consisting of NI data acquisition cards, LEM voltage and current sensors, and a laptop, was developed, as shown in Fig. 3. The total energy consumed in an SLM process includes coating energy and building energy. The coating energy is affected by the number of layers, which is determined by build height and layer thickness.

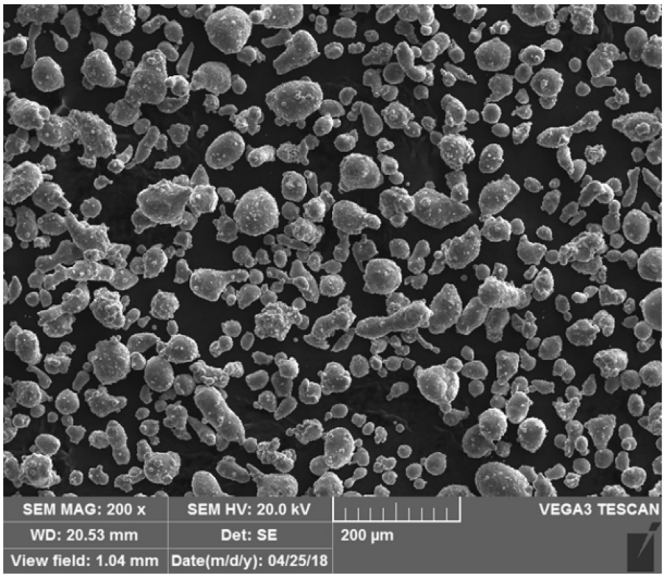


**Fig. 2.** An SEM image of the AlSi10Mg powder in use.

**Table 1**
Chemical compositions of the AlSi10Mg powder in use.

| Elements | Al | Si | Mg | Fe | Cu | Mn | Zn | Ti | Ni | Pb | Sn |
|---|---|---|---|---|---|---|---|---|---|---|---|
| Wt.% | Balance | 9.5 | 0.38 | 0.18 | <0.01 | <0.01 | <0.01 | <0.01 | <0.01 | <0.01 | <0.01 |

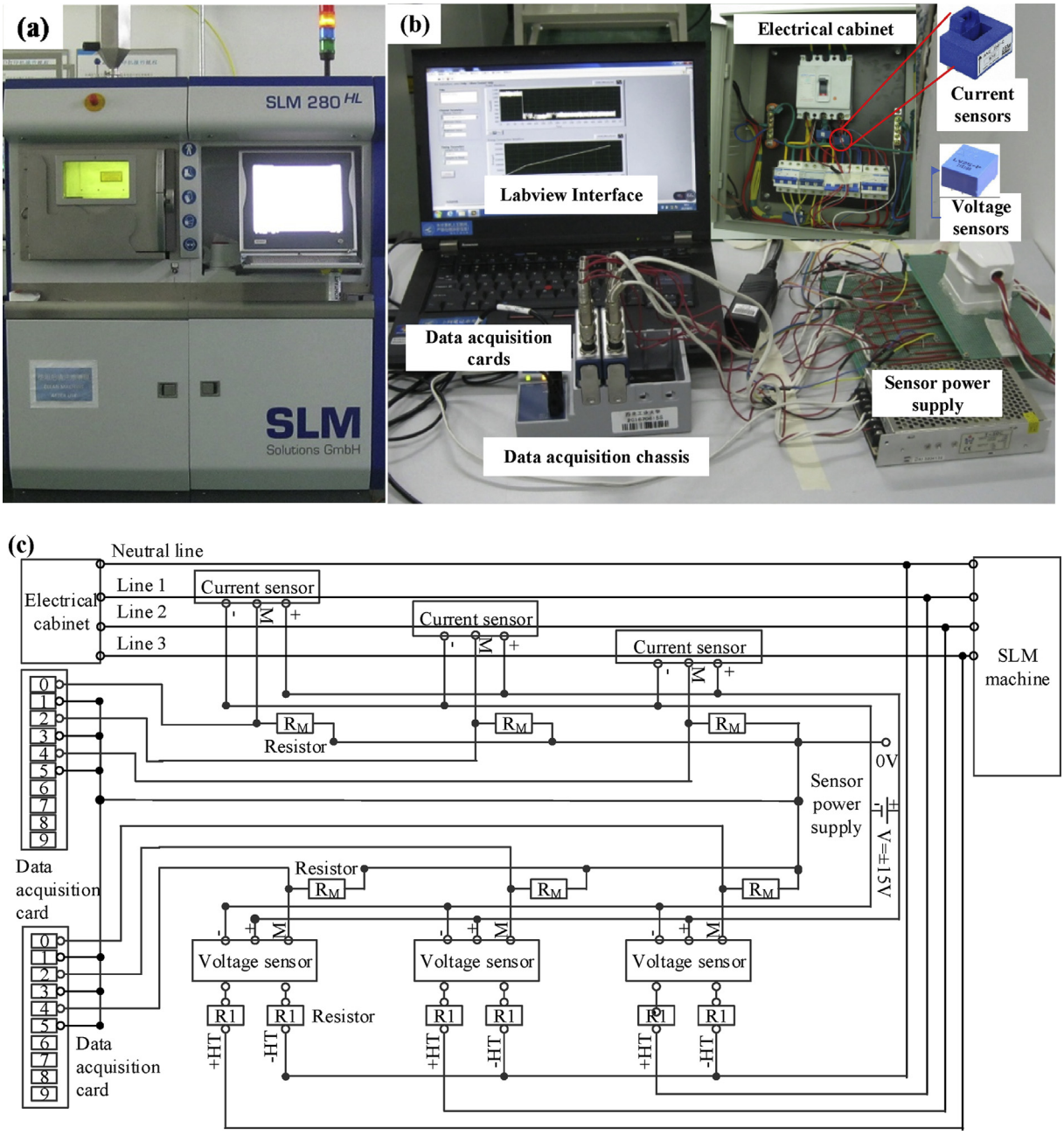


**Fig. 3.** Experimental set-up: (a) SLM machine, (b) energy data acquisition equipment and (c) schematic circuit diagram for energy data recording.

Comparably, building energy is responsible for the behavior of grain growth and the quality of the fabricated parts (Liu et al., 2018a). It is, thereby, focused in this study.

Specific energy consumption (SEC) $E_s$ [J/kg] is used for evaluating energy consumption. It is expressed as:

$$E_S = \frac{E_{build}}{m_{build}} \tag{3}$$

where $E_{build}$ is the electrical energy consumed during a part building process [J], and $m_{build}$ is the weight of a fabricated part [kg]. The building energy $E_{build}$can be calculated as the sum of energy consumed by laser and auxiliary components of a SLM machine:

$$E_{build} = E_{laser} + E_{aux} = (P_L + P_A) \cdot t_{scan} \tag{4}$$

where $E_{laser}$ and $E_{aux}$ are the energy consumed by laser and auxiliary system during a building process [J], respectively; $P_L$ and $P_A$ are the power consumption of laser and auxiliary system [W], respectively; $t_{scan}$ is the total scanning time [s], which can be calculated as:

$$t_{scan} = \frac{1000 V_{build}}{\dot{v}} \tag{5}$$

where $V_{build}$ is the volume of a fabricated part [$cm^3$], $\dot{v}$ is build-up rate [$mm^3/s$]. The build-up rate $\dot{v}$ can be calculated as:

$$\dot{v} = \frac{n \cdot t_{layer} \cdot h_{space} \cdot v_{scan}}{10^6} \tag{6}$$

where $n$ is the number of working lasers, $t_{layer}$ is layer thickness [μm], $h_{space}$is hatch distance [μm], $v_{scan}$ is scan speed [mm/s]. $m_{build}$ is then calculated as:

$$m_{build} = \frac{\rho_p \cdot V_{build}}{1000} \tag{7}$$

where $\rho_p$is part density [$g/cm^3$]. Substituting Equations (4)–(7) into Equation (3), the $E_S$ [J/kg] is calculated as:

$$E_S = \frac{10^6 (P_L + P_A)}{n \cdot \rho_p \cdot t_{layer} \cdot h_{space} \cdot v_{scan}} \tag{8}$$

Both $P_A$ and $P_L$ can be obtained through experiments, $P_A$ can be considered as a constant, and $P_L$ can be estimated as a linear function of laser output power:

$$P_L = n \cdot \left( P_f + \frac{P_{laser}}{\eta} \right) \tag{9}$$

where $P_f$is the fixed power consumption of laser system [W], $\eta$ is laser efficiency, which usually ranges between 10 and 30%, depending on the laser type (Lee et al., 2017),$P_{laser}$is laser output power [W]. The hatch distance is calculated as:

$$h_{space} = W(1 - O) \tag{10}$$

where $W$ is the width of a single track [μm], $O$ is overlap rate.

Here, we propose an index to represent energy effectiveness, which is defined as the ratio between equivalent quality and energy consumption per kilogram of part produced, expressed as:

$$E_I = \frac{\overline{Q}}{\overline{E}_S} \tag{11}$$

where $\overline{Q}$and $\overline{E}_S$are the normalized values of quality $Q$ and SEC $E_S$, respectively. They are described as:

$$\begin{cases} \overline{Q} = \dfrac{Q}{Q_{\max}} \\ \overline{E}_S = \dfrac{E_S}{E_{S\min}} \end{cases} \tag{12}$$

where $Q_{\max}$and $E_{S\min}$ mean the maximum part quality and minimum specific energy consumption, expressed as:

$$\begin{cases} Q_{\max} = \max\{Q_1, Q_2, ..., Q_k\} \\ E_{S\min} = \min\{E_{S,1}, E_{S,2}, ..., E_{S,k}\} \end{cases} \tag{13}$$

where $k$ is the number of experimental runs. The value of $E_I$is no greater than 1. The closer the value of $E_I$ is to 1, the better the energy effectiveness is. In the case of multiple quality indicators, a composite energy effectiveness indicator is defined as:

$$E_{I,C} = \frac{1}{m} \sum_{i=1}^{m} E_{I,i} \tag{14}$$

where $m$ is the number of quality indicators.

### 3.2. Experiment design

Different combinations of process parameters were used to investigate the $E_{I,C}$ of SLM processes. The layer thickness was fixed at 30 μm. The process parameters, laser power, scan speed and overlapping rate, were considered as variables in a full factorial design.

First, single track experiments were conducted to study the influence of different parameter sets on melt track width, as shown in Table 2. A total of 36 groups of experiments were conducted. The processing condition for each sample made in single tracks was repeated at least three times. The morphology of the tracks was observed and the width of single track was measured three times for each processing condition.

Then, single layer experiments were conducted to determine the process window of overlapping ratio. Single layers were produced with four levels of overlap rates (0.2, 0.25, 0.3 and 0.35) at the laser power of 320 W and scan speed of 750 mm/s. The size of single layer was designed to be 8 mm × 8 mm, and the surface morphology observations of single layer were repeated three times for each processing condition.

After that, multiple layer experiments were conducted to test the porosity, hardness and tensile strength of the parts manufactured with various combinations of process parameters (see Table 3). Processing conditions for the multiple layers were selected on the basis that the tracks in the single layer are well-connected. For each combination of parameters, three cubic bulk samples with a dimension of 8 mm × 6 mm × 10 mm and one cuboid sample with a dimension of 10 mm × 52 mm × 14.5 mm were produced. A total of 81 cubic bulk samples were manufactured to investigate the influence of process parameters on the porosity and hardness of the samples (see Fig. 4 (a)). A total of 27 cuboid samples were manufactured to make tensile examples, as shown in Fig. 4 (b). The samples were cut from the substrate by electrical discharge machining (EDM). Each cuboid bulk part was further cut into three samples for tensile strength testing, are shown in Fig. 5. In all cases of multiple layer samples, measurements were conducted three times for each processing condition and the average values of density, tensile strength and hardness were reported.

Finally, the energy consumption of the SLM machine were online measured, and the SEC values using different parameter combinations were calculated according to Equation (8).

**Table 2**
Process parameters for the single-track experiments.

| Levels | 1 | 2 | 3 | 4 | 3 | 4 |
|---|---|---|---|---|---|---|
| Laser power [W] | 300 | 320 | 340 | 360 | 380 | 400 |
| Scan speed[mm/s] | 300 | 450 | 600 | 750 | 900 | 1050 |

**Table 3**
Process parameters for the multiple layer experiments.

| Levels | 1 | 2 | 3 |
|---|---|---|---|
| Laser power [W] | 320 | 360 | 400 |
| Scan speed[mm/s] | 600 | 750 | 900 |
| Overlap rate [%] | 25 | 30 | 35 |

## 4. Results

### 4.1. Results of quality and energy consumption

Fig. 6 shows the surface morphologies of single tracks fabricated with various laser power and scan speeds. Good consolidation is characterized by the continuous tracks with laser power ranging 320–400 W and scan speed ranging 600–900 mm/s. The surface of single track was getting unstable at scan speed over 1100 mm/s or laser power less than 300 W.

For single track, better energy effectiveness means forming continuous regular straight line with lower laser power and faster speed. However, beyond certain values, it could lead to unstable and irregular tracks, because the powders cannot absorb sufficient energy to melt completely, which initiate balling effect. In our tests, laser power $\geq$320 W and scan speed $\leq$900 mm/s was acceptable.

The widths of stable single tracks were measured, which varied from 102.9 μm to 155.2 μm (see Fig. 7). The track width increases with the increase of laser power and the decrease of scan speed. With these data, hatch distances were calculated using Equation (10).

Fig. 8 depicts the images of single layers fabricated with four levels of overlap rates. All of them can form proper single layers, except 20% overlapping ratio. The neighbor tracks failed to achieve a sound interconnection with an overlap rate of 0.2. When the overlap rate increases to 0.3 and 0.35, the tracks were regular and

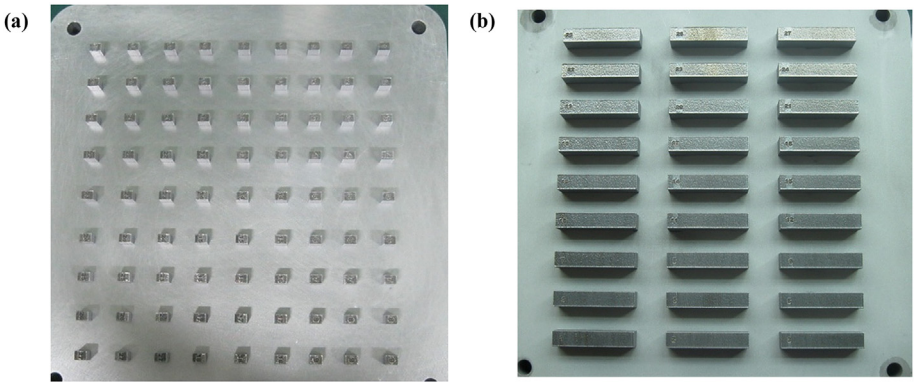


**Fig. 4.** The samples manufactured by SLM process (a) cubic bulk samples and (b) cuboid samples.

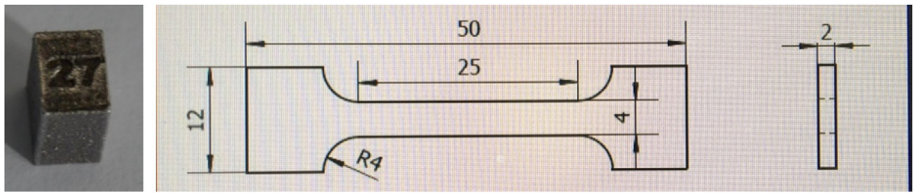


**Fig. 5.** Sample for porosity, hardness and tensile strength testing.

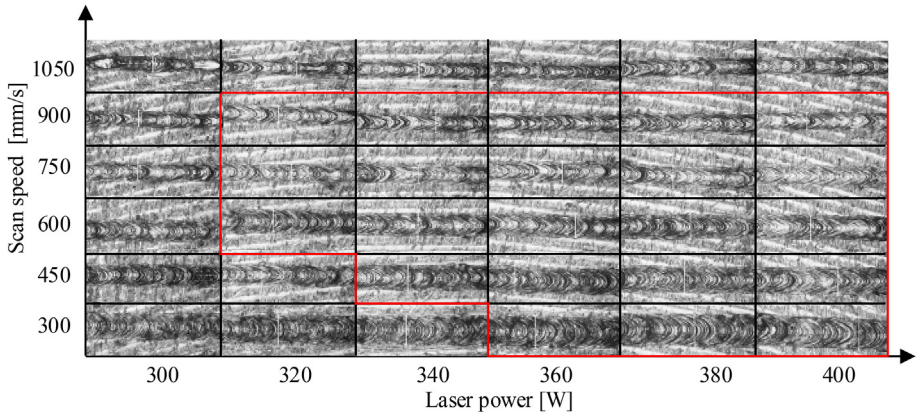


**Fig. 6.** Surface morphologies of the single-track samples fabricated by SLM process with laser power ranging from 300 to 400 W and scan speed ranging from 300 to 1050 mm/s. The samples in the red wireframe are continuous and stable single tracks. (For interpretation of the references to colour in this figure legend, the reader is referred to the Web version of this article.)

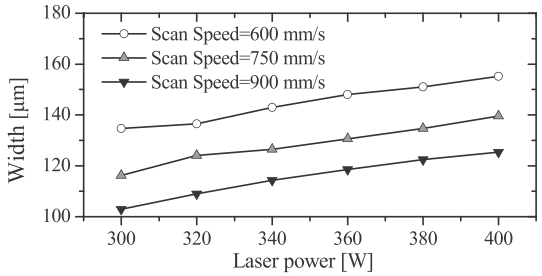


**Fig. 7.** Width of the single tracks versus scan speed of the laser beam for different power.

well-connected to form a dense and smooth surface of single layer. As a result, the overlap rates ranging from 0.25 to 0.35 were selected. The results of the quality of the SLM processed AlSi10Mg samples is summarized in Table 4.

The measured power consumption of an SLM process is shown in Fig. 9. The power fluctuates due to the intermittently running of water-cooling unit and laser. The average auxiliary power consumption $P_A = 1925$ W, when the water-cooling unit is off, otherwise, $P_A = 3665$ W. During a building process, the water-cooling unit is turned on and off repeatedly, and the time spent in each state accounts for a fixed percentage of total build time. As shown in Fig. 9 (a), the time spent by the water-cooling unit in the off mode and working mode were 284 s and 114 s, respectively, during one cycle. In this case, the auxiliary power consumption $P_A$ can be calculated as:

$$P_A = (1925 \times 284 + 3665 \times 114)/(114 + 284) = 2423 \text{ W} \quad (15)$$

In Fig. 9 (b), power fluctuates due to the frequently switching on and off of heater. The laser power consumption was identified by subtracting idle power from the laser-operating power. Various laser output power and corresponding consumption was measured, as shown in Table 5. Based on the measured data, the laser power consumption was modeled using linear regression:

$$P_L = n\,(129.46 + 2.52\,P)\,(R^2 = 0.998) \quad (16)$$

In this case, two lasers were working together ($n = 2$). Substituting Equations 15 and 16 into Equation (8), the values of SEC can be calculated, as show in the last column of Table 4.

### 4.2. Joint analysis of quality and SEC

The contribution and effects of process parameters on the quality and SEC are further investigated, as shown in Fig. 10. Relative density decreases with increased laser power and deceased scan speed, and reaches the highest at an overlap rate of 0.3. The tensile strength is significantly affected by laser power and overlap rate. It increases with an increase of overlap rate and decreases with an increase of laser power and scan speed. A reduction in the scan speed and an increase in the overlap rate both have a positive effect on energy delivered into the material, which will lead to an improvement of part consolidation, and eventually an improvement of tensile strength. We also notice that hardness increases and then decreases by increasing laser power and overlap rate. By increasing scan speed, hardness decreases. Scan speed and overlap rate strongly affect SEC. The overlap rate has an increasing effect while the scan speed has a decreasing effect. Because the energy consumption in fabricating samples is also related to building time. SEC slightly decreases with an increase of laser power, because the hatch distance increases in the meantime, which leads to a reduced building time.

To investigate the interaction effect of process parameters on the quality performances and SEC, the contour plots were drawn using the data in Table 4, by varying the two different process parameters and keeping the third parameter at the middle level. Fig. 11 (a) shows that high relative density can be achieved at the middle levels of laser power, scan speed and overlap rate. Higher tensile strength is achieved at lower laser power and scan speed and higher overlap rate (see Fig. 11 (b)). As seen from Fig. 11 (c), by increasing laser power and overlap rate, hardness increases and then reduces. Fig. 11 (d) describes that the SEC increases when scan speed decreases and overlap rate increases.

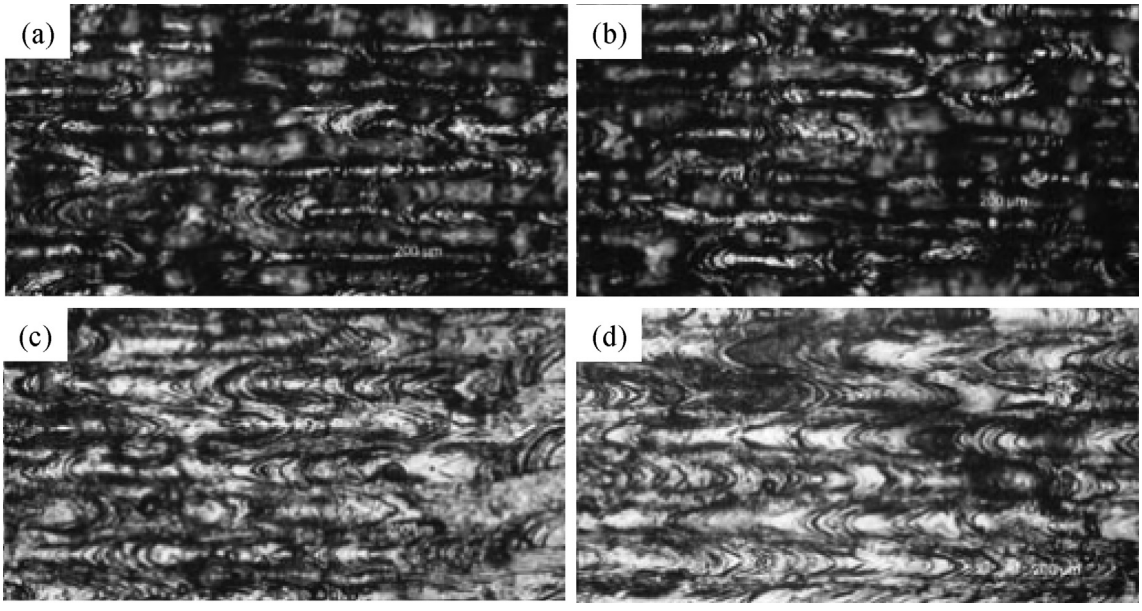


**Fig. 8.** Optical images of the surface morphologies of SLM-processed AlSi10Mg single layers. The process parameters are: laser power: 320 W, scan speed: 750 mm/s and overlap rate at: (a) 0.2, (b) 0.25, (c) 0.3 and (d) 0.35.

**Table 4**
Results of the quality performances and SEC of the SLM processed AlSi10Mg samples.

| No | Laser Power [W] | Scan speed [mm/s] | Hatch distance [μm] | Overlap rate | Density [g/cm$^3$] | Relative density | Tensile strength [MPa] | Hardness [HV] | SEC [MJ/kg] | EE of relative density | EE of tensile strength | EE of hardness | Comprehensive EE |
|---|---|---|---|---|---|---|---|---|---|---|---|---|---|
| 1 | 320 | 600 | 102.4 | 0.25 | 2.6102 | 0.9739 | 455.00 | 119.0 | 446.33 | 0.7828 | 0.7891 | 0.6746 | 0.7488 |
| 2 | 320 | 600 | 95.5 | 0.3 | 2.6266 | 0.9801 | 450.00 | 123.2 | 475.59 | 0.7393 | 0.7324 | 0.6554 | 0.7091 |
| 3 | 320 | 600 | 88.7 | 0.35 | 2.6270 | 0.9802 | 443.33 | 130.8 | 511.97 | 0.6869 | 0.6703 | 0.6464 | 0.6679 |
| 4 | 320 | 750 | 93.1 | 0.25 | 2.6196 | 0.9774 | 448.33 | 124.4 | 391.33 | 0.8961 | 0.8868 | 0.8043 | 0.8624 |
| 5 | 320 | 750 | 86.9 | 0.3 | 2.6094 | 0.9737 | 443.33 | 123.2 | 420.88 | 0.8300 | 0.8154 | 0.7406 | 0.7953 |
| 6 | 320 | 750 | 80.7 | 0.35 | 2.6204 | 0.9777 | 445.00 | 127.8 | 451.32 | 0.7772 | 0.7632 | 0.7165 | 0.7523 |
| 7 | 320 | 900 | 81.8 | 0.25 | 2.6310 | 0.9817 | 443.33 | 127.6 | 369.54 | 0.9531 | 0.9286 | 0.8736 | 0.9185 |
| 8 | 320 | 900 | 76.3 | 0.3 | 2.6221 | 0.9784 | 446.67 | 127.8 | 397.53 | 0.8830 | 0.8698 | 0.8134 | 0.8554 |
| 9 | 320 | 900 | 70.9 | 0.35 | 2.6298 | 0.9813 | 450.00 | 122.6 | 426.55 | 0.8254 | 0.8166 | 0.7272 | 0.7897 |
| 10 | 360 | 600 | 111.0 | 0.25 | 2.5965 | 0.9688 | 431.67 | 127.2 | 433.35 | 0.8021 | 0.7711 | 0.7427 | 0.7719 |
| 11 | 360 | 600 | 103.6 | 0.3 | 2.6237 | 0.9790 | 436.67 | 135.2 | 459.49 | 0.7644 | 0.7356 | 0.7445 | 0.7482 |
| 12 | 360 | 600 | 96.2 | 0.35 | 2.6063 | 0.9725 | 441.67 | 116.4 | 498.14 | 0.7004 | 0.6863 | 0.5912 | 0.6593 |
| 13 | 360 | 750 | 98.0 | 0.25 | 2.6083 | 0.9732 | 430.00 | 129.8 | 390.90 | 0.8932 | 0.8515 | 0.8402 | 0.8616 |
| 14 | 360 | 750 | 91.4 | 0.3 | 2.6308 | 0.9817 | 441.67 | 123.2 | 415.54 | 0.8476 | 0.8228 | 0.7502 | 0.8068 |
| 15 | 360 | 750 | 84.9 | 0.35 | 2.6087 | 0.9734 | 445.00 | 128.8 | 451.14 | 0.7741 | 0.7635 | 0.7224 | 0.7533 |
| 16 | 360 | 900 | 88.9 | 0.25 | 2.6092 | 0.9736 | 420.00 | 119.0 | 358.97 | 0.9731 | 0.9057 | 0.8388 | 0.9058 |
| 17 | 360 | 900 | 83.0 | 0.3 | 2.6260 | 0.9799 | 431.67 | 127.2 | 382.02 | 0.9202 | 0.8747 | 0.8425 | 0.8791 |
| 18 | 360 | 900 | 77.1 | 0.35 | 2.6252 | 0.9795 | 446.67 | 122 | 411.38 | 0.8542 | 0.8405 | 0.7504 | 0.8150 |
| 19 | 400 | 600 | 116.4 | 0.25 | 2.5618 | 0.9559 | 420.00 | 118.6 | 437.63 | 0.7836 | 0.7429 | 0.6857 | 0.7374 |
| 20 | 400 | 600 | 108.6 | 0.3 | 2.6241 | 0.9791 | 445.00 | 131.0 | 457.92 | 0.7671 | 0.7522 | 0.7238 | 0.7477 |
| 21 | 400 | 600 | 100.9 | 0.35 | 2.6296 | 0.9812 | 438.33 | 139.2 | 491.84 | 0.7157 | 0.6899 | 0.7161 | 0.7072 |
| 22 | 400 | 750 | 104.7 | 0.25 | 2.6056 | 0.9722 | 430.00 | 124.8 | 382.68 | 0.9114 | 0.8698 | 0.8251 | 0.8688 |
| 23 | 400 | 750 | 97.7 | 0.3 | 2.6164 | 0.9763 | 431.67 | 127.4 | 408.41 | 0.8576 | 0.8182 | 0.7893 | 0.8217 |
| 24 | 400 | 750 | 90.7 | 0.35 | 2.5981 | 0.9694 | 446.67 | 120.8 | 443.03 | 0.7850 | 0.7804 | 0.6899 | 0.7518 |
| 25 | 400 | 900 | 94.1 | 0.25 | 2.6250 | 0.9795 | 416.67 | 125.4 | 352.20 | 0.9978 | 0.9158 | 0.9009 | 0.9381 |
| 26 | 400 | 900 | 87.8 | 0.3 | 2.5864 | 0.9651 | 443.33 | 113.2 | 383.11 | 0.9038 | 0.8958 | 0.7476 | 0.8491 |
| 27 | 400 | 900 | 81.5 | 0.35 | 2.6152 | 0.9758 | 438.33 | 118.4 | 408.18 | 0.8577 | 0.8313 | 0.7339 | 0.8076 |

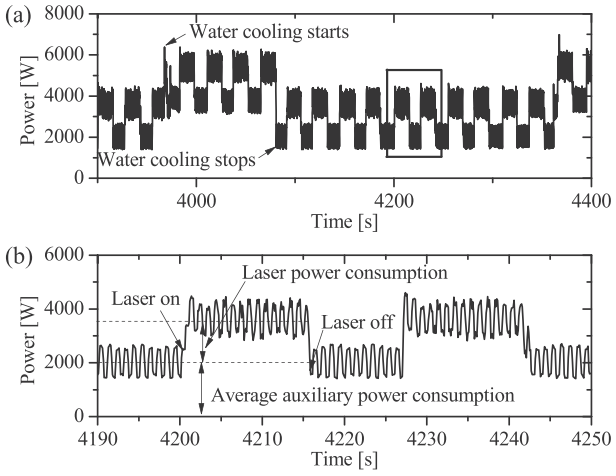


**Fig. 9.** Measured power in the SLM process of AlSi10Mg samples, (a) power consumption of the SLM machine during part fabricating process; (b) enlarged area of the black box in (a).

### 4.3. Results of energy effectiveness analysis

Joint analysis of SEC and quality is shown in Fig. 12. The relative density shows no clear trends with increased SEC. The maximum relative density of 0.9817 was achieved at the SEC of 369.5 MJ/kg. As for tensile strength and hardness, increasing trends could be observed with increased SEC. However, samples with higher SEC do not necessarily have high tensile strength or hardness. The maximum tensile strength of 455 MPa and hardness of 139.2 HV were achieved at the SEC of 446.33 MJ/kg and 491.84 MJ/kg, respectively. The Pareto fronts of the experimental results are marked with dotted circles (see Fig. 12). The experiment No. 7 and 25 in Table 4 were the Pareto fronts for all combinations of SEC and quality indicators. It can be inferred that better EE can be achieved in these two experiments.

Using Equations 11–14, the EE for relative density, tensile strength and hardness were calculated, as shown in Table 4. Two highest values of composite EE were achieved for experiment No. 25 (0.9381) and No. 7 (0.9185), which agrees with the results illustrated in Fig. 12.

To analyze the influences of process parameters on the energy effectiveness, main plot effect graphs are drawn, as shown in Fig. 13. Upon increasing the scan speed from 600 to 900 mm/s or decreasing overlap rate from 0.35 to 0.25, the values of EE increase. Such trends are opposite to those of SEC in Fig. 10 (d). In Fig. 10, the variations of SEC are greater than those of the relative density, tensile strength and hardness. As a result, the trends of EE are largely determined by those of SEC. In Fig. 13, the steep lines indicate that increasing the scan speed or decreasing overlap rate could lead to great improvements in EE. In comparison, the values of EE vary slightly with an increase of laser power, indicating that increasing laser power does not effectively improve the energy effectiveness.

The interactions of process parameters on EE are further analyzed, as shown in Fig. 14. The contour plots are drawn using the calculated EE data shown in Fig. 12. Overall, the EE increases with

**Table 5**
Power consumption of a single laser operating at various output power levels.

| Output power [W] | 40 | 80 | 120 | 160 | 200 | 240 | 280 | 320 | 360 | 400 |
|---|---|---|---|---|---|---|---|---|---|---|
| Power consumption [W] | 227.9 | 329.1 | 438.1 | 513.4 | 633.5 | 755.3 | 844.8 | 948.3 | 1023.6 | 1130.0 |

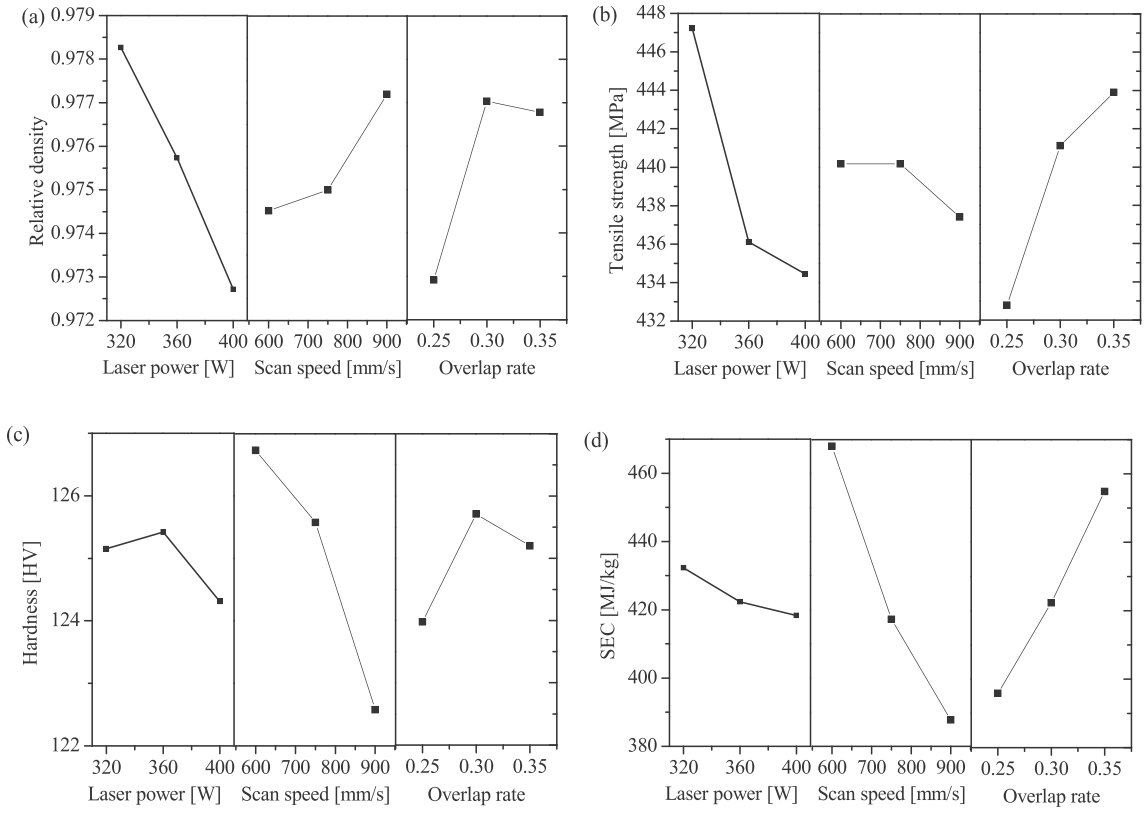


**Fig. 10.** Main effect plots of laser power, scan speed and overlap rate for (a) relative density, (b) tensile strength, (c) hardness and (d) SEC.

an increasing scan speed and decreasing overlap rate, and the influence of laser power on the EE is insignificant.

The above results indicate that there is a large potential to reduce energy consumption while meet part quality requirements via process parameter configuration. Larger scan speed and lower overlap rate are recommended to reduce energy consumption. For instance, with the quality requirements of relative density $\geq$0.98, tensile strength $\geq$440 MPa and hardness $\geq$120 HV, the scan speed of 900 mm/s, overlap rate of 0.25 and laser power of 320 W can be configured to reduce energy consumption. In this case, the quality requirements are satisfied and the SEC of 369.54 MJ/kg is achieved, which is 27.8% lower than the SEC value when the scan speed of 600 mm/s, overlap rate of 0.35 and laser power of 320 W are used.

## 5. Discussions

From the above results, the highest relative density was achieved at the laser power of 360 W, scan speed of 750 mm/s and overlap rate of 0.3, which agrees with the results in literature (Yap et al., 2016). The tensile strength increases with decreasing laser power and scan speed and increasing overlap rate, while the maximum hardness is obtained at the middle levels of laser power and overlap rate.

Comparing the results shown in Figs. 11 and 14, it can be seen that the improvement of quality with increased EE differs. On one hand, EE can be improved without significantly sacrificing quality performances, such as density and hardness. On the other hand, improving EE will greatly reduce the quality performances, such as tensile strength. Because when the EE increases with an increase in scan speed and decrease in overlap rate, the tensile strength decreases. Therefore, to optimize EE with acceptable quality performances is complicated. The comparison of EE and related quality are plotted as presented in Fig. 15.

Fig. 15 (a) shows that achieving high density could lead to low EE for some samples due to the high energy demand (experiment No. 3). It is possible to achieve both high EE and density simultaneously by carefully selecting process parameters (experiment No. 25). The high tensile strength is achieved at moderate levels of EE (experiment Nos. 1, 2, 9, 18 and 24) (see Fig. 15 (b)), and the higher EE is related to lower tensile strength (experiment Nos. 16 and 25). Therefore, it is not recommended to save energy without considering the tensile strength of the samples. The higher hardness is achieved with lower EE (experiment Nos. 11 and 21) and higher EE is related to moderate hardness (see Fig. 15 (c)) (experiment Nos. 7 and 25). Thus, to achieve an acceptable hardness, energy can be saved.

In industrial applications, besides the density, tensile strength and hardness studied in this paper, other quality indicators, such as surface roughness, dimensional accuracy and fatigue also need to be studied. The effective reduction of energy consumption while fulfilling the quality requirements is another problem.

In this work, AlSi10Mg is primarily considered, so the findings may be limited to AlSi10Mg. The EE of many commercially used materials, such as Ti6Al4V, 316L and 18Ni-300 are not concluded. The quality is studied based on the as-built samples. When post-processing, e.g. heat treatment is applied, the quality might change (Gu et al., 2019), which needs further investigation. In that case, the energy consumed in heat treatment also needs to be taken into account. Layer thickness could also impact greatly on energy and part quality, which is set constant in this study. Furthermore, the research was conducted on an SLM 280 $^{HL}$ machine. The results might be influenced by machines with different energy characteristics (Zhu et al., 2019).

Environmental performance, such as carbon footprint, green

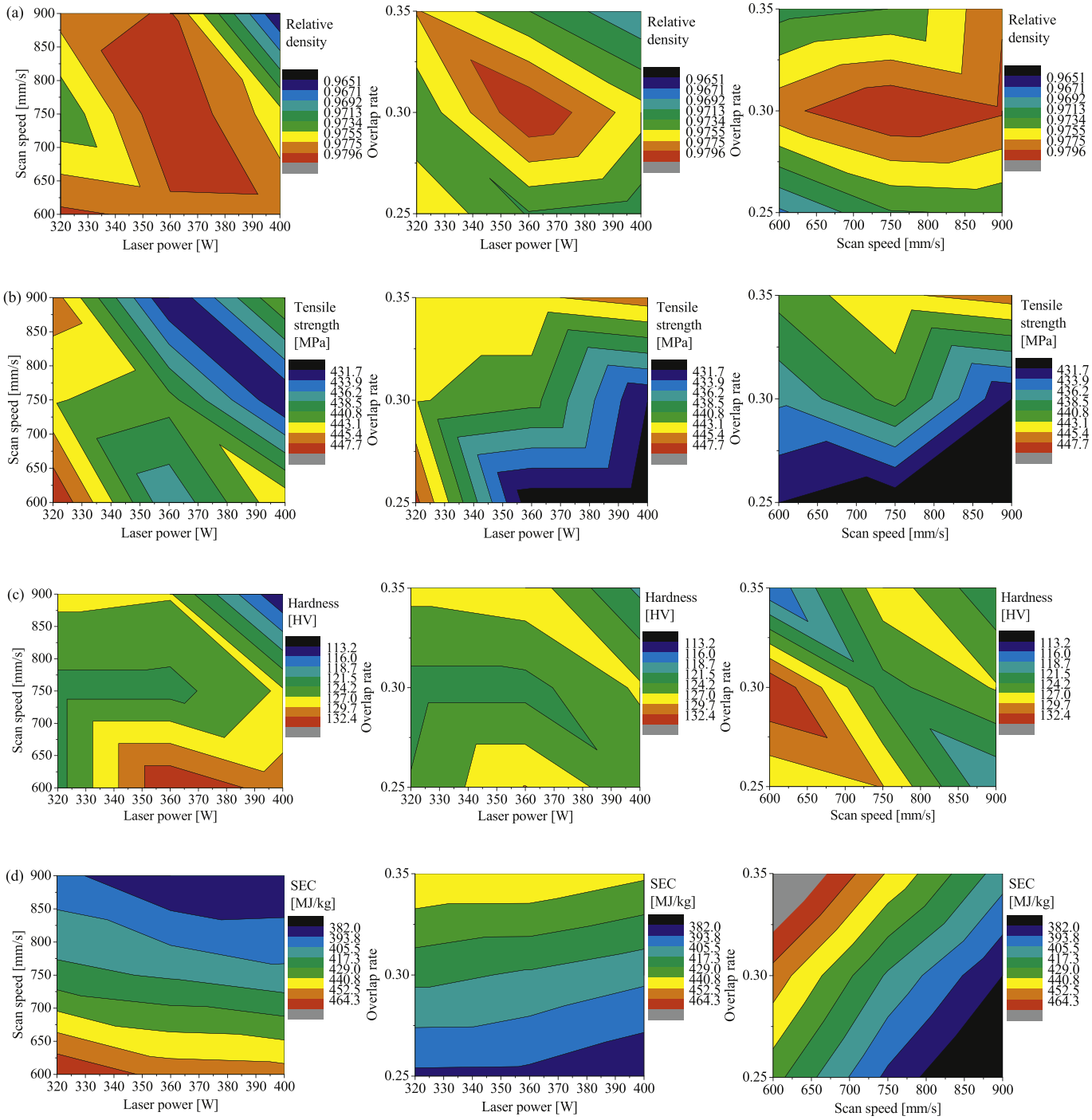


**Fig. 11.** Contour plots for (a) relative density, (b) tensile strength, (c) hardness and (d) SEC.

performance and sustainability, needs to be considered in the AM process design and production planning stage. On the one hand, parameter selection with consideration of quality and energy consumption, i.e. energy effectiveness, could help an operator to make better and long-term sustainable decisions. On the other hand, more sustainability-related issues could be considered in the adoption and further innovation of AM technologies. AM technologies can produce parts with application-specific quality and consume a right amount of electrical energy by selecting appropriate process parameters, adopting less energy-intensive AM technologies and developing more energy-efficient AM machines. Technologies being used in recent years to increase the energy efficiency of AM process include higher powered lasers and multiple lasers. Thus, both part quality and energy consumption need to be considered in the design, adoption and development of more environmentally-benign AM technologies. As a result, parts with satisfied quality performances could be produced by AM technologies with less energy consumption.

## 6. Conclusions

This study demonstrates the possibility of reducing the

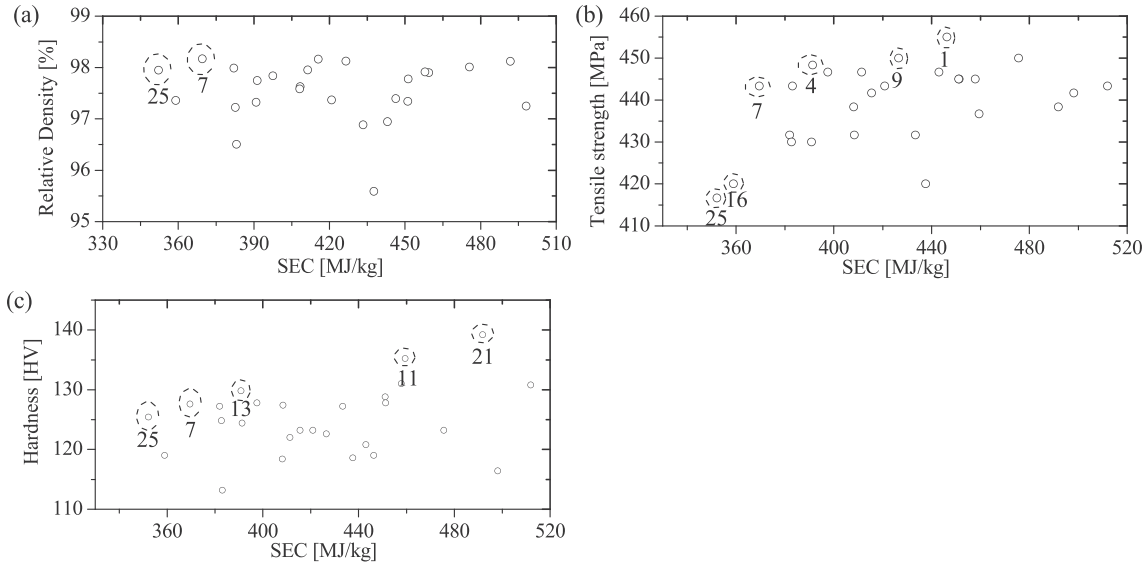


**Fig. 12.** Joint analysis of SEC and quality of the SLM processed AlSi10Mg samples with different combinations of process parameters: (a) SEC versus relative density, (b) SEC versus tensile strength and (c) SEC versus hardness. The Pareto fronts of the experimental results are marked with dotted circles. The number below the dotted circle refers to the experiment number as shown in Table 4.

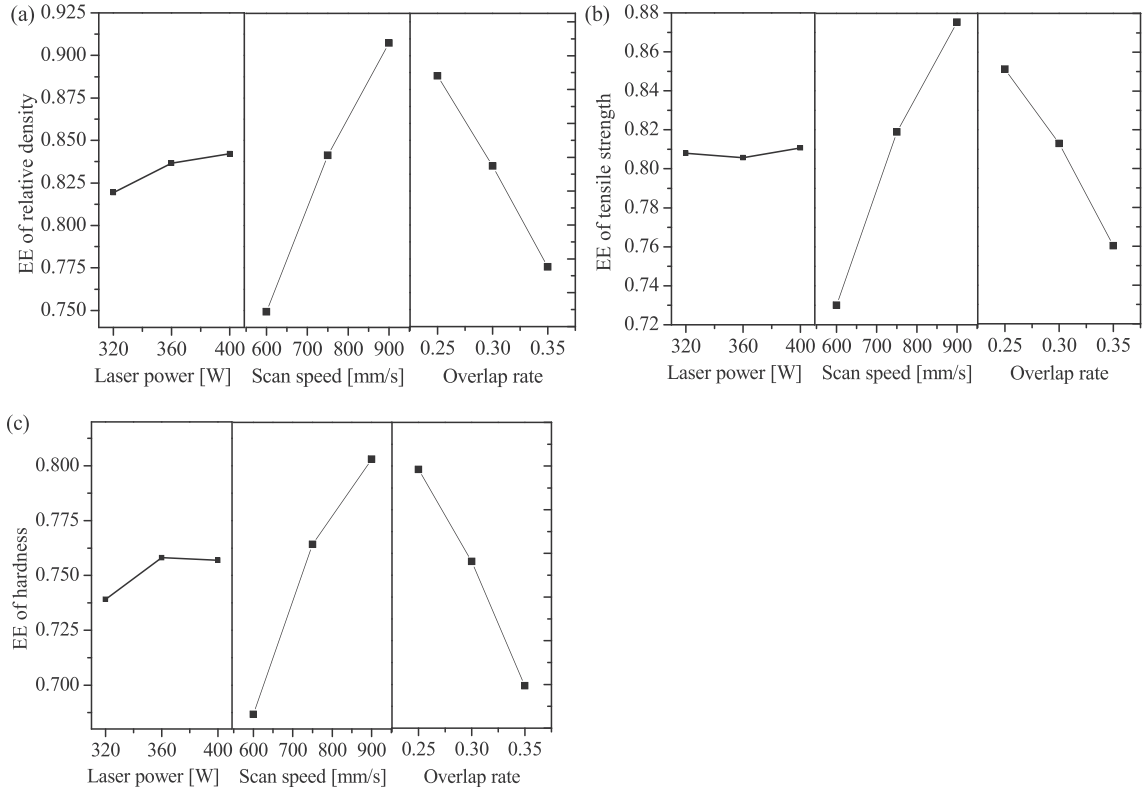


**Fig. 13.** Main effect plots of laser power, scan speed and overlap rate for EE of (a) relative density, (b) tensile strength and (c) hardness.

electrical energy without significantly sacrificing the part quality. We systematically investigate the effect of process parameters on density, tensile strength, hardness, energy consumption and EE of the parts fabricated by SLM process. The primary conclusions are summarized as follows:

(1) The suitable process parameters of laser power ranging from 320 to 400 W, scan speed ranging from 600 to 900 mm/s and overlap rate ranging from 0.25 to 0.35 with which the tracks can achieve good consolidation and sound interconnections are selected in the single track and single layer experiments.
(2) Higher tensile strength can be achieved by higher overlap rate, lower laser power and scan speed. The density

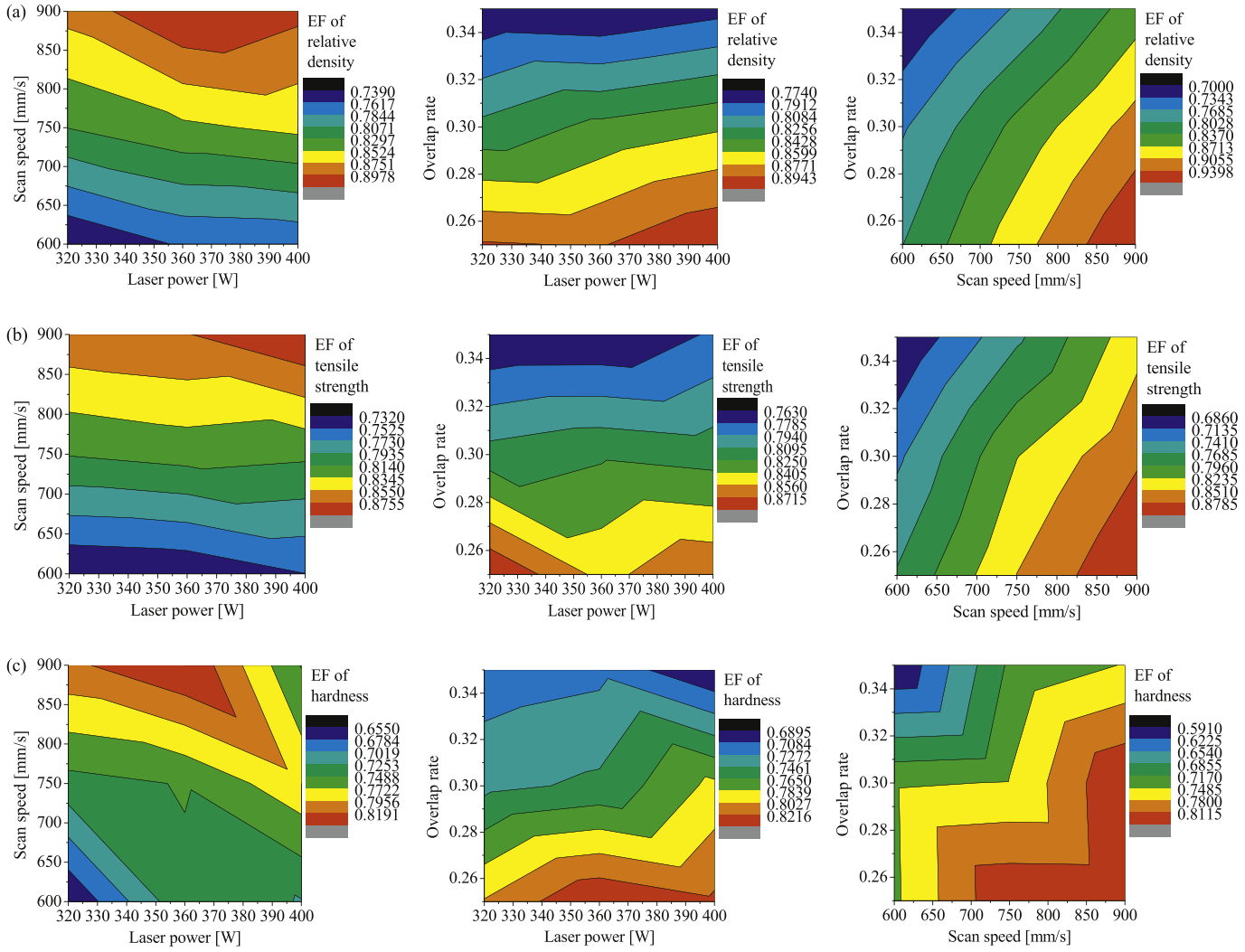


**Fig. 14.** Contour plots for the EE of (a) relative density, (b) tensile strength and (c) hardness.

decreases with increased laser power and decreased scan speed while the hardness decreases with increased scan speed. The SEC increases with an increased overlap rate and decreased scan speed.

(3) The EE increases with an increase of scan speed and decrease of overlap rate. The influence of laser power on the EE is not significant.

(4) The improvement of EE depends on the selection of process parameters. EE can be reduced without significantly sacrificing density and hardness, while improving EE will greatly reduce the tensile strength. High tensile strength can be achieved at moderate levels of EE and energy can be saved when the EE is high to achieve a moderate hardness.

(5) There is a great potential for energy reduction while not compromising the quality performances through carefully selecting process parameters in the process design stage.

This paper presents a first step towards energy-effective AM research, where the many opportunities remain open. The concept of EE proposed in this research can be used to improve the environmental performance of AM part at the product and process design stages. In the design stage, the EE and mechanical properties of different materials can be estimated and the materials with highest EE while satisfying the quality requirements can be selected. In the process design stage, the machines and process parameters can be selected to increase the EE, thereby reducing the energy consumption of parts during the manufacturing stage.

The limitation of this work is that only the possibilities of improving EE with the constraint of quality requirements through process parameter configuration were discussed. Further research will be conducted on the optimization of EE and quality of actual functional parts by integrating design and process parameters.

## CRediT authorship contribution statement

**Tao Peng:** Conceptualization, Methodology, Resources, Investigation, Writing - review & editing, Funding acquisition, Supervision. **Jingxiang Lv:** Software, Validation, Formal analysis, Data curation, Writing - original draft, Visualization. **Arfan Majeed:** Investigation. **Xihui Liang:** Writing - review & editing.

## Declaration of competing interest

The authors declare that they have no known competing financial interests or personal relationships that could have appeared to influence the work reported in this paper.

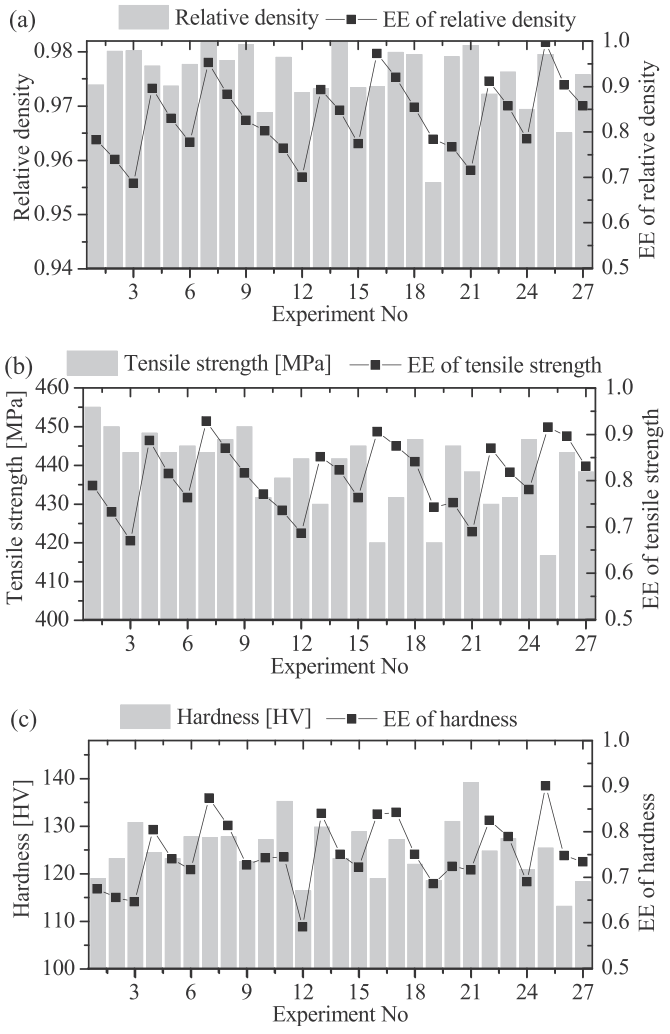


**Fig. 15.** Quality and EE of (a) relative density, (b) tensile strength and (c) hardness.

## Acknowledgements

This work was supported by the National Natural Science Foundation of China (No. 51705428), Natural Science Foundation of Zhejiang Province (No. LY19E050019), Natural Science Basic Research Program of Shaanxi (Program No. 2020JQ-380), the International Clean Energy Talent Program (iCET) of China Scholarship Council (Liujinfa[2017]5047 and Liujinfa[2018]5023) and the Fundamental Research Funds for the Central Universities, CHD (No. 300102250303).

## References

Aboulkhair, N.T., Simonelli, M., Parry, L., Ashcroft, I., Tuck, C., Hague, R., 2019. 3D printing of Aluminium alloys: additive Manufacturing of Aluminium alloys using selective laser melting. Prog. Mater. Sci. 106, 100578.
Ahmed, N., 2019. Direct metal fabrication in rapid prototyping: a review. J. Manuf. Process. 42, 167–191.
Anwar, A.B., Pham, Q.-C., 2017. Selective laser melting of AlSi10Mg: effects of scan direction, part placement and inert gas flow velocity on tensile strength. J. Mater. Process. Technol. 240, 388–396.
Bai, S.G., Perevoshchikova, N., Sha, Y., Wu, X.H., 2019. The effects of selective laser melting process parameters on relative density of the AlSi10Mg parts and suitable procedures of the Archimedes method. Applied Sciences-Basel 9 (3), 583.
Baumers, M., Tuck, C., Hague, R., Ashcroft, I., Wildman, R., 2010. A comparative study of metallic additive manufacturing power consumption. In: Proceedings of the 2010 Solid Freeform Fabrication Symposium. The University of Texas at Austin, Austin, TX, 9-11 August.
Baumers, M., Tuck, C., Bourell, D.L., Sreenivasan, R., Hague, R., 2011. Sustainability of additive manufacturing: measuring the energy consumption of the laser sintering process. Proc. IME B J. Eng. Manufact. 225 (12), 2228–2239.
Bourhis, F.L., Kerbrat, O., Hascoet, J.-Y., Mognol, P., 2013. Sustainable manufacturing: evaluation and modeling of environmental impacts in additive manufacturing. Int. J. Adv. Manuf. Technol. 69 (9), 1927–1939.
Delgado, J., Ciurana, J., Rodríguez, C.A., 2012. Influence of process parameters on part quality and mechanical properties for DMLS and SLM with iron-based materials. Int. J. Adv. Manuf. Technol. 60 (5), 601–610.
EIA, 2016. Energy Consumption by Sector. www.eia.gov/totalenergy/data/monthly/pdf/sec2_3.pdf. assessed 15.05.16.
Gao, W., Zhang, Y., Ramanujan, D., Ramani, K., Chen, Y., Williams, C.B., Wang, C.C.L., Shin, Y.C., Zhang, S., Zavattieri, P.D., 2015. The status, challenges, and future of additive manufacturing in engineering. Comput. Aided Des. 69, 65–89.
Garavaglia, M., Demir, A.G., Zarini, S., Victor, B.M., Previtali, B., 2019. Process development and coaxial sensing in fiber laser welding of 5754 Al-alloy. J. Laser Appl. 31 (2), 043129.
Gu, X.H., Zhang, J.X., Fan, X.L., Dai, N.W., Xiao, Y., Zhang, L.C., 2019. Abnormal corrosion behavior of selective laser melted AlSi10Mg alloy induced by heat treatment at 300 degrees C. J. Alloys Compd. 803, 314–324.
Gupta, A.K., Lloyd, D.J., Court, S.A., 2001. Precipitation hardening in Al–Mg–Si alloys with and without excess Si. Mater. Sci. Eng., A 316 (1), 11–17.
Gutowski, T., Dahmus, J., Thiriez, A., 2006. Electrical Energy Requirements for Manufacturing Processes, 13th CIRP International Conference on Life Cycle Engineering, pp. 623–627. Leuven, Belgium.
Jiang, H.-Z., Li, Z.-Y., Feng, T., Wu, P.-Y., Chen, Q.-S., Feng, Y.-L., Li, S.-W., Gao, H., Xu, H.-J., 2019. Factor analysis of selective laser melting process parameters with normalised quantities and Taguchi method. Optic Laser. Technol. 119, 105592.
Kellens, K., Yasa, E., Renaldi, Dewulf, W., Kruth, J.P., Duflou, J.R., 2011. Energy and resource efficiency of SLS/SLM processes. SFF Symposium 1–16.
Kellens, K., Renaldi, R., Dewulf, W., Kruth, J.P., Duflou, J.R., 2014. Environmental impact modeling of selective laser sintering processes. Rapid Prototyp. J. 20 (6), 459–470.
Kruth, J.P., Froyen, L., Van Vaerenbergh, J., Mercelis, P., Rombouts, M., Lauwers, B., 2004. Selective laser melting of iron-based powder. J. Mater. Process. Technol. 149 (1), 616–622.
Lee, H., Lim, C.H.J., Low, M.J., Tham, N., Murukeshan, V.M., Kim, Y.-J., 2017. Lasers in additive manufacturing: a review. Int. J. Precis Eng Manuf-Green Technol. 4 (3), 307–322.
Liu, P.W., Ji, Y.Z., Wang, Z., Qiu, C.L., Antonysamy, A.A., Chen, L.Q., Cui, X.Y., Chen, L., 2018a. Investigation on evolution mechanisms of site-specific grain structures during metal additive manufacturing. J. Mater. Process. Technol. 257, 191–202.
Liu, Z., Jiang, Q., Ning, F., Kim, H., Cong, W., Xu, C., Zhang, H.-c., 2018b. Investigation of energy requirements and environmental performance for additive manufacturing processes. Sustainability 10 (10), 3606.
Luo, Y., Ji, Z., Leu, M.C., Caudill, R., 1999. Environmental performance analysis of solid freedom fabrication processes. In: Proceedings of the 1999 IEEE International Symposium on Electronics and the Environment (Cat. No.99CH36357), pp. 1–6.
Lv, J., Peng, T., Tang, R., 2019. Energy modeling and a method for reducing energy loss due to cutting load during machining operations. Proc. IME B J. Eng. Manufact. 233 (3), 699–710.
Lv, J., Peng, T., Zhang, Y., Wang, Y., 2020. A novel method to forecast energy consumption of selective laser melting processes. Int. J. Prod. Res. 1–17 https://doi.org/10.1080/00207543.2020.1733126.
Majeed, A., Lv, J., Peng, T., 2019. A framework for big data driven process analysis and optimization for additive manufacturing. Rapid Prototyp. J. 25 (2), 308–321.
Park, H.-S., Nguyen, T.-T., Dang, X.-P., 2016. Energy-Efficient optimization of forging process considering the manufacturing history. Int. J. Precis Eng Manuf-Green Technol. 3 (2), 147–154.
Paul, R., Anand, S., 2012. Process energy analysis and optimization in selective laser sintering. J. Manuf. Syst. 31 (4), 429–437.
Peng, T., Chen, C., 2018. Influence of energy density on energy demand and porosity of 316L stainless steel fabricated by selective laser melting. Int. J. Precis. Eng. Manuf. Green Technol. 5 (1), 55–62.
Peng, T., Kellens, K., Tang, R., Chen, C., Chen, G., 2018a. Sustainability of additive manufacturing: an overview on its energy demand and environmental impact. Addit. Manuf. 21, 694–704.
Peng, T., Xu, S., Zhang, H., Zhu, Y., 2018b. Influence of exposure time on energy consumption and mechanical properties of SLM fabricated parts. Rapid Prototyp. J. 24 (9), 1428–1435.
Peng, S., Li, T., Zhao, J., Lv, S., Tan, G.Z., Dong, M., Zhang, H., 2019a. Towards energy and material efficient laser cladding process: modeling and optimization using a hybrid TS-GEP algorithm and the NSGA-II. J. Clean. Prod. 227, 58–69.
Peng, T., Zhu, Y., Yang, Y., Zhang, H., 2019b. Energy effectiveness in additive manufacturing using design for property. Procedia CIRP 80, 132–137.
Perevoshchikova, N., Rigaud, J., Sha, Y., Heilmaier, M., Finnin, B., Labelle, E., Wu, X., 2017. Optimisation of selective laser melting parameters for the Ni-based superalloy IN-738 LC using Doehlert's design. Rapid Prototyp. J. 23 (5), 881–892.
Ratnadeep, P., Sam, A., 2015. A combined energy and error optimization method for metal powder based additive manufacturing processes. Rapid Prototyp. J. 21 (3), 301–312.
Read, N., Wang, W., Essa, K., Attallah, M.M., 2015. Selective laser melting of

AlSi10Mg alloy: process optimisation and mechanical properties development. Mater. Des. 65, 417–424.
Sadowski, M., Ladani, L., Brindley, W., Romano, J., 2016. Optimizing quality of additively manufactured Inconel 718 using powder bed laser melting process. Addit. Manuf. 11, 60–70.
Strano, G., Hao, L., Everson, R.M., Evans, K.E., 2013. A new approach to the design and optimisation of support structures in additive manufacturing. Int. J. Adv. Manuf. Technol. 66 (9), 1247–1254.
Tan, X., Kok, Y., Tan, Y.J., Descoins, M., Mangelinck, D., Tor, S.B., Leong, K.F., Chua, C.K., 2015. Graded microstructure and mechanical properties of additive manufactured Ti–6Al–4V via electron beam melting. Acta Mater. 97, 1–16.
Trevisan, F., Calignano, F., Lorusso, M., Pakkanen, J., Aversa, A., Ambrosio, E., Lombardi, M., Fino, P., Manfredi, D., 2017. On the selective laser melting (SLM) of the AlSi10Mg alloy: process, microstructure, and mechanical properties. Materials 10 (1), 76.
Winter, M., Li, W., Kara, S., Herrmann, C., 2014. Determining optimal process parameters to increase the eco-efficiency of grinding processes. J. Clean. Prod. 66, 644–654, 0.
Yap, C.Y., Chua, C.K., Dong, Z.L., 2016. An effective analytical model of selective laser melting. Virtual Phys. Prototyp. 11 (1), 21–26.
Yi, L., Krenkel, N., Aurich, J.C., 2018. An energy model of machine tools for selective laser melting. Procedia CIRP 78, 67–72.
Yi, L., Ravani, B., Aurich, J.C., 2019. Development of a simulation tool for predicting energy consumption of selective laser melting by using MATLAB/Simulink. Procedia CIRP 81, 28–33.
Zeng, Y.D., Li, T.H., Deng, Y.L., Yuan, C., 2019. A general empirical energy consumption model for computer numerical control milling machine. J. Manuf. Sci. Eng.Transactionsering.ASME 141 (2), 021020.
Zhang, L., Zhang, S., Zhu, H., Hu, Z., Wang, G., Zeng, X., 2018. Horizontal dimensional accuracy prediction of selective laser melting. Mater. Des. 160, 9–20.
Zhang, J., Song, B., Wei, Q., Bourell, D., Shi, Y., 2019a. A review of selective laser melting of aluminum alloys: processing, microstructure, property and developing trends. J. Mater. Sci. Technol. 35 (2), 270–284.
Zhang, S., Rauniyar, S., Shrestha, S., Ward, A., Chou, K., 2019b. An experimental study of tensile property variability in selective laser melting. J. Manuf. Process. 43, 26–35.
Zheng, J., Huang, B.B., Zhou, X.J., 2018. A low carbon process design method of sand casting based on process design parameters. J. Clean. Prod. 197, 1408–1422.
Zhu, Y., Peng, T., Jia, G., Zhang, H., Xu, S., Yang, H., 2019. Electrical energy consumption and mechanical properties of selective-laser-melting-produced 316L stainless steel samples using various processing parameters. J. Clean. Prod. 208, 77–85.